The Structural Design of Tall and Special Buildings

Deformability design of high-performance concrete beams

Journal:	*The Structural Design of Tall and Special Buildings*
Manuscript ID:	TAL-11-0027.R1
Wiley - Manuscript type:	Research Article
Date Submitted by the Author:	n/a
Complete List of Authors:	Ho, Johnny; The University of Hong Kong, Civil Engineering
Keywords:	Beams, Curvature, Deformability, High-performance materials, High-strength concrete, High-strength steel, Plastic hinge, Reinforced Concrete, Rotation capacity, Strength

Abstract: The use of high-performance materials (HPM) such as high-strength concrete (HSC) and high-strength steel (HSS) is becoming more popular in the construction of beams and columns of tall buildings. These HPM not only increase the stiffness and decrease the strength-to-weight ratio, but also provide a more sustainable construction method by minimising the construction materials needed. However, HSC and HSS are more brittle than normal-strength concrete and steel respectively. Therefore, it will adversely affect the deformability of concrete beams. To evaluate the pros and cons of adopting HPM in beam design, the author will investigate the flexural strength and deformability of concrete beams made of HPM. The deformability in this study is expressed in normalised rotation capacity and investigated by a parametric study using nonlinear moment-curvature analysis taking into account the degree of reinforcement, confining pressure, concrete and steel yield strength. From the results, it is evident that the deformability of concrete beams increases as the degree of reinforcement decreases or confining pressure increases. However, the effects of concrete and steel yield strength depend on other factors. For practical design purpose, charts and formulas are produced for designing high-performance concrete beams to meet with specified flexural strength and deformability requirement.

Deformability design of high-performance concrete beams

Johnny Ching Ming Ho[1]

Abstract

The use of high-performance materials (HPM) such as high-strength concrete (HSC) and high-strength steel (HSS) is becoming more popular in the construction of beams and columns of tall buildings. These HPM not only increase the stiffness and decrease the strength-to-weight ratio, but also provide a more sustainable construction method by minimising the construction materials needed. However, HSC and HSS are more brittle than normal-strength concrete and steel respectively. Therefore, it will adversely affect the deformability of concrete beams. To evaluate the pros and cons of adopting HPM in beam design, the author will investigate the flexural strength and deformability of concrete beams made of HPM. The deformability in this study is expressed in normalised rotation capacity and investigated by a parametric study using nonlinear moment-curvature analysis taking into account the degree of reinforcement, confining pressure, concrete and steel yield strength. From the results, it is evident that the deformability of concrete beams increases as the degree of reinforcement decreases or confining pressure increases. However, the effects of concrete and steel yield strength depend on other factors. For practical design purpose, charts and formulas are produced for designing high-performance concrete beams to meet with specified flexural strength and deformability requirement.

Keywords: Beams; Curvature; Deformability; High-performance materials; High-strength concrete; High-strength steel; Plastic Hinge; Reinforced concrete; Rotation capacity; Strength

[1] Assistant Professor, Department of Civil Engineering, The University of Hong Kong, Hong Kong. (Tel.: (852) 28591966; Fax: (852) 25595337; email: johnny.ho@hku.hk)

1. Introduction

High-performance materials such as high-strength concrete (HSC) and high-strength steel (HSS) have been popularly used in the construction of tall buildings structures because of its improved strength-to-weight ratio and stiffness. It also provides a more sustainable construction method by lowering the embodied energy and carbon level in the structures (Bilodeau and Malhotra 2000; Scrivener and Kirkpatrick 2008; Xu *et al*. 2008) through reducing the amount of materials used for the same structural loads when compare with traditional low strength materials such as normal-strength concrete (NSC) and normal-strength steel (NSS). More importantly, HSC is characterised by its reduced permeability and hence improve the durability of the concrete structures. This is because of the better packing density contributed by ultra-fine materials or fillers like meta-kaolin, micro-silica, slags and super-fine cement (Wong and Kwan 2008; Kwan and Wong 2008). Accordingly, HSC is often being adopted in various structural members in tall buildings as well as in water-retaining and maritime structures.

Apart from HSC, HSS with yield strength higher than 500 MPa is also increasingly adopted as longitudinal and confining reinforcement in concrete members (Restrepo *et al*. 2006). The use of HSS is getting more popular and is allowed by most of the current RC design codes. For example, Eurocode 2 (2004) and NZS3101 (2006) allows the use of steel with maximum yield strength of 600 and 800 MPa respectively. The major advantage of HSS is that it provides the same strength with a smaller steel area, which relieves the steel congestion problem at lap splice locations and beam-column joints. When HSS is adopted as confining steel within the critical regions (Pam and Ho 2009) of columns, it provides the same confining pressure with larger spacing.

Despite these advantages, HSC and HSS are more brittle than NSC and NSS respectively. When beam section with HSS is significantly under-reinforced, it would fracture at large inelastic curvature (Ho *et al*. 2005; Bai and Au 2009). As confinement, HSS may not develop full yield strength at low and moderate axial load, in particular when HSC is adopted, which exhibits less dilation at maximum moment capacity. Evidently, the design of structures consisting of HPM (e.g. HSC and HSS) should not

be treated the same as that of structures consisting of traditional materials. For these high-performance structures, special consideration should be placed on reinforcement detailing and confining steel provision such that plastic hinge can be developed and moment redistribution can occur during extreme events (Lu 2009; Nam *et al*. 2009; Weerheijm *et al*. 2009). This will avoid abrupt failure of structures without ample warning (Wu *et al*. 2004; Lam *et al*. 2008; Teran-gilmore *et al*. 2010).

From performance-based design point of view, the design of sufficient flexural deformability and ductility is essential (Englekirk 2008; Fry *et al*. 2009; Goel *et al*. 2009; Yousuf and Bagchi 2009; Zareian *et al*. 2010). This is because adequate deformability can ensure that the maximum limit of deformation during servicing stage will not be exceeded, and hence the integrity of the structures is maintained. On the other hand, adequate ductility can prevent immediate collapse of structures during extreme events, such as earthquake or accidental impact, when the maximum limit of deformability has been accidentally exceeded. Although structural damage may occur and eventually the buildings may need to be reconstructed, the safety of the occupants is successfully protected.

The author has previously carried out studies on the ductility of NSC and HSC beams and columns (Ho *et al*. 2003; Lam *et al*. 2008). From these studies, it has been found the ductility of concrete beams can be increased by decreasing the degree of reinforcement, adding compression steel and increasing concrete strength a constant tension steel ratio. It can also be enhanced by providing sufficient confining pressure to the concrete core within critical region in the following ways by: (1) Confining the concrete member using circular or rectangular hollow steel tube (Ellobody and Young 2006; Choi *et al.* 2008; Park *et al.* 2008; Feng and Young 2009, 2010; Jiang *et al*. 2010). (2) Using external steel plate (Sabouri-Ghomi *et al*. 2008; Su *et al.* 2009). (3) Wrapping the concrete member with fibre reinforced polymer (Lam and Teng 2009; Hong *et al.* 2010; Wu and Wei 2010), (4) Installing sufficient transverse reinforcement provided to plastic hinge region for concrete core confinement (Ho and Pam 2003; Havaei and Keramati 2009; Yan and Au 2009; Ho 2011). These methods are commonly adopted in the design of low to medium rise buildings. For very tall building structures, the huge amount of energy induced by earthquake can in addition be

dissipated by installing dampers (Chung *et al*. 2009; Heo *et al*. 2009; Lee *et al*. 2009; Marano and Greco 2009; Chen and Han 2010) and adopting base isolation (Ribakov 2009; Takewaki and Fujita 2009; Yamamoto *et al*. 2009).

From design point of view, current method of design for beams in non-seismic region focuses on the provision of sufficient flexural strength than deformability. Also, the concept of ductility is not able to reveal the actual deformation capacity of the members. Therefore, in the performance-based design approach, adequate deformability should also be considered instead of just adequate ductility, as provided in the past. However, currently the provision of flexural deformability is deemed-to-comply by some empirical rules controlling the maximum tension steel area or neutral axis depth. This has been proven to provide satisfactory deformability to concrete beams consisting of NSC and/or NSS in non-seismic region (Park and Ruitong 1988, Kwan *et al*. 2006). However, for RC beams containing HSC and/or HSS, as well as those located in regions of low to moderate seismicity such as Hong Kong, the design for sufficient deformability to cater for the imposed seismic demand (Tsang *et al*. 2009) should be considered on top of providing sufficient flexural strength. Since the required deformability provided to these beams in low to moderate seismicity is larger than that in non-seismic regions, the existing deemed-to-comply rules can no longer be applied.

Apart from the above, the existing deemed-to-comply rules cannot provide a consistent deformability to concrete beams made of high-strength concrete (HSC) and/or high-strength steel (HSS). Since the deformability decreases as concrete strength and steel yield strength increase because of the increased materials' brittleness, the existing deemed-to-comply rules will decrease the deformability provided to beams with HSC and/or HSS. More critically, the deformability will decrease to an unacceptably low level if very brittle ultra-HSC is adopted. Considering nowadays the increasing popularity of using HSC and HSS, which are more cost effective and environmentally friendly, the existing empirical rules should be reformed for deformability design of RC beams to incorporate the adoption of HSC and/or HSS.

In this paper, the critical factors affecting the deformability of concrete beams will be investigated by normalised rotation capacity. From the results, two methods for

designing deformability and flexural strength of concrete beams are developed. The first method is to use design chart, which plot the deformability against flexural strength for different beam sections. For designing singly-reinforced concrete beams, a simpler method, which evaluates the possible range of tension steel ratios based on two inequalities, is advocated. For practical application, numerical examples for designing concrete beams in non-seismic regions (i.e. smaller deformability demand) and in low to moderate seismicity regions (i.e. larger deformability demand) are given.

2. Nonlinear moment-curvature analysis

The deformability of RC beams is studied using the method of nonlinear moment-curvature analysis developed previously by the authors (Pam *et al.* 2001; Ho *et al.* 2003). The stress-strain curves of concrete by Attard and Setunge (1996) were adopted and that of steel reinforcement follows the model of Eurocode 2 (EC2 2004) incorporating stress-path dependence during the unloading stage. The unloading path is having the same initial elastic modulus until it reaches zero steel stress. The stress-strain curves of concrete and steel are shown in Fig 1.

There were five assumptions made in the analysis: (1) Plane sections before bending remain plane after bending. (2) The tensile strength of the concrete may be neglected. (3) There is no relative slip between concrete and steel reinforcement. (4) The concrete core is confined while the concrete cover is unconfined. (5) The confining pressure provided to the concrete core by confinement is assumed to be constant throughout the concrete compression zone. Assumptions (1) to (4) are commonly accepted and have been adopted by various researchers (Au *et al*. 2009; Bai and Au 2009; Lam *et al*. 2009; Kwak and Kim 2010). Assumption (5) is not exact but nevertheless a fairly reasonable assumption (Ho *et al*. 2010). In the analysis, the moment-curvature curve of the beam section is analysed by applying prescribed curvatures incrementally starting from zero. At a prescribed curvature, the stresses developed in the concrete and the steel are determined from their stress-strain curves. Then, the neutral axis depth and resisting moment are evaluated from equilibrium conditions. The above procedure is repeated until the resisting moment has increased to

the peak and then decreased to below 80% of the peak moment. Fig 2 describes a typical beam sections adopted in the nonlinear moment-curvature analysis. However, it should be noted that the nonlinear moment-curvature analysis, which is a section analysis method, is not able to model the effect of steel buckling. However, this effect will be significantly only for doubly RC beams with large spacing of confining steel that are not very common in practical design. The method is not able to reveal the effect of concrete shrinkage (Gribniak *et al*. 2008; Kaklauskas *et al*. 2008) as well. Therefore the results obtained in this study tends to be slightly conservative.

3. Flexural deformability analyses

3.1 Flexural deformability analysis

In this study, the flexural deformability of beam sections are expressed in terms of normalised rotation capacity θ_{pl} defined as follows (Zhou *et al*. 2010):

$$\theta_{pl} = \phi_u d \tag{1}$$

where ϕ_u is the ultimate curvature, d is the effective depth. The ultimate curvature is taken as the curvature when the resisting moment has dropped to $0.8M_p$ after reaching M_p, where M_p is the peak moment. The value of θ_{pl} represents the rotation capacity of beam assuming that the plastic hinge length ℓ_p is equal to effective depth. For concrete beams subjected to flexure without axial load, it is reasonable because the plastic hinge length of concrete beams is found to remain relatively constant at about $0.4d$ to $0.6h$ (Mendis 2001; EC2 2004; NZS3101 2006) from the maximum bending moment point. Since the plastic hinge length varies slightly with the content of longitudinal steel, confining steel as well as concrete strength, the actual rotation capacity may be slightly different from the normalised rotation capacity. In such a circumstance, the actual rotation capacity of the concrete beam can be obtained by multiplying the normalised rotation capacity with ℓ_p/d.

A comprehensive parametric study on the effects of various factors on the deformability has been conducted previously (Zhou *et al*. 2010). It has been observed that the major factors influencing the deformability of concrete beams are: (1) Degree of reinforcement (Eq. 4); (2) Concrete strength; (3) Steel area ratios (defined as steel area divided by the effective area of beam section); (4) Steel yield strength; and (5) Confining pressure. The beam sections analysed in the parametric study has been shown in Figure 2. The concrete strength f_{co} was varied from 40 to 100 MPa. The confining pressure f_r evaluated as per Mander *et al*. (1988) was varied from 0 to 4 MPa. The tension steel ratio ρ_t was varied from 0.4 to 2 times the balanced steel ratio, the compression steel ratio ρ_c was varied from 0 to 2%. The tension f_{yt} and compression f_{yc} steel yield strength were varied from 400 to 800 MPa.

3.2 Failure modes and balanced steel ratio

The balanced steel ratio of a beam section is defined as the area of tension steel that causes the steel to yield during failure. It is defined as $\rho_{bo} = A_{sb}/bd$, where A_{sb} is the balanced steel area. For beam section with tension steel area less than ρ_{bo}, the steel will yield during failure and the section is under-reinforced. Otherwise, the steel will not yield and the section is over-reinforced. For beam sections with also compression steel ratio ρ_c, the balanced steel ratio ρ_b is given by:

$$\rho_b = \rho_{bo} + (f_{yc} / f_{yt})\rho_c \tag{2}$$

The values of ρ_{bo} for various concrete strengths and confining pressure can be determined from first principle using nonlinear moment-curvature analysis by iterating the tension steel ratio such that the steel yields (Ho *et al*. 2003), and are shown in Tables 1 to 3 for f_{yt} = 400, 600 and 800 MPa and f_r = 0, 1, 2, 3 and 4 MPa. It can also be evaluated using the following empirical equation:

$$\rho_{bo} = 0.005\left(f_{co}\right)^{0.58}\left(1+1.2f_r\right)^{0.3}(f_{yt}/460)^{-1.35} \tag{3}$$

All strengths are in MPa, 400 MPa $\le f_{yt} \le$ 800 MPa and $0 \le f_r \le 4$ MPa.

3.3 Degree of reinforcement, tension and compression steel

The deformability of concrete beams is determined by the degree of section being under- or over-reinforced, which can be quantitatively evaluated by the degree of reinforcement λ expressed in Eq. (4):

$$\lambda = \frac{f_{yt}\rho_t - f_{yc}\rho_c}{f_{yt}\rho_{bo}} \quad (4)$$

The beam section is classified as under-reinforced, balanced and over-reinforced sections when λ is less than, equal to and larger than 1.0 respectively. Fig 3a plots the variation of deformability of concrete beams (in θ_{pl}) against λ for different concrete strength. It is seen that at constant concrete strength, the deformability decreases as λ increases until reaching 1.0. After that, the deformability remains constant. Also, it is evident that at a given λ, the deformability decreases as the concrete strength increases because of the reduced materials' ductility performance. However, if concrete strength is increased at the same tension steel ratio ρ_t, it can be seen from Fig 3b that the deformability increases as concrete strength increases albeit that HSC is less deformable *per se*. This is because the balanced steel ratio increases as concrete strength increases (Eq. 3), and hence λ decreases for a given ρ_t and the deformability increases. Therefore, the effect of concrete strength on deformability is dependent on other factors such as the degree of reinforcement and tension steel ratio.

The addition of compression steel is always beneficial to the improvement of deformability because it will increase the balanced steel ratio as per Eq. (2), and at the same time decrease the numerator of λ as shown in Eq. (4). Both of these reduce the value of λ at a particular concrete strength and tension steel ratio. Accordingly, the deformability of increases as compression steel ratio increases.

3.4 Effects of yield strength of tension f_{yt} and compression steel f_{yc}

The effects of yield strength of tension steel on deformability of concrete beams are shown in Fig 4. Figs 4a and 4b plot the deformability against λ and ρ_t respectively for various f_{yt} = 400, 600 and 800 MPa. From Fig 4a, it is evident that the increase in tension steel yield strength at the same degree of reinforcement will increase the deformability of concrete beams. Therefore, the use of HSS as tension steel will improve the deformability of concrete beam at a given λ. However, as seen in Fig 4b, the use of HSS as tension steel will decrease the deformability of concrete beam at a given ρ_t. This is because increasing f_{yt} at a given ρ_t and concrete strength f_{co} will decrease the value of λ and hence the deformability of the concrete beam.

The effects of yield strength of compression steel on deformability of concrete beams are shown in Fig 5. Figs 5a and 5b plot the deformability against λ and ρ_t respectively for various f_{yc} = 400, 600 and 800 MPa. From Fig 5a, it is evident that the increase in compression steel yield strength at the same degree of reinforcement will not affect significantly the deformability of concrete beams. Therefore, the use of HSS as compression steel will neither improve nor decrease the deformability of concrete beam at a given λ. However, as seen in Fig 5b, the use of HSS as compression steel will improve significantly the deformability of concrete beam at a given ρ_t. This is because increasing f_{yc} at a given ρ_t and concrete strength f_{co} will decrease the value of λ and hence increase the deformability of the concrete beam.

3.5 Effects of confining pressure

To study the effect of the confining pressure f_r, θ_{pl} is plotted against confining pressures f_r for different concrete strength f_{co}, degree of reinforcement λ and tension steel ratios ρ_t in Fig 6. The confining pressure is evaluated according to the method proposed by Mander *et al.* (1988) taking into account the arching action of concrete between laterally restrained longitudinal steel. The formulas are re-written as follows:

$$f_r = 0.5 k_e \rho_s f_{ys} \quad (5a)$$

$$f_{cc} = f_{co}\left(-1.254 + 2.254\sqrt{1 + \frac{7.94 f_r}{f_{co}}} - 2\frac{f_r}{f_{co}}\right) \quad (5b)$$

where f_{cc} is the enhanced concrete strength due to confinement and k_e is the confinement effectiveness factor. It is evident from Fig 6(a) that at a given λ, θ_{pl} increases as the f_r increases for all concrete strength. It is also seen from Fig 6(b) that at a fixed f_{co}, θ_{pl} increases as f_r increases for all λ. In Fig 6(c), it is seen that at a fixed f_{co}, θ_{pl} increases as the confining pressure f_r increases for all ρ_t. On the whole, the addition of confining pressure is always beneficial to the deformability improvement of concrete beams.

3.6 Formulas for direct evaluation of deformability

The following formulas were derived previously by the authors (Zhou *et al*. 2010) for direct evaluation of deformability of NSC and HSC beams.

$$\theta_{pl} = 0.03m(f_{co})^{-0.3}(\lambda)^{-1.0n}\left(1+110(f_{co})^{-1.1}\left(\frac{f_{yc}\rho_c}{f_{yt}\rho_t}\right)^3\right)\left(\frac{f_{yt}}{460}\right)^{0.3} \quad (6a)$$

$$m = 1+4f_{co}^{\ 0.4}(f_r / f_{co}) \quad (6b)$$

$$n = 1+3f_{co}^{\ 0.2}(f_r / f_{co}) \quad (6c)$$

To verify the validity of the above formulas, the flexural deformability predicted by Eq. (6) has been compared with the rotation capacities of concrete beams obtained experimentally for NSC beams (Nawy *et al.* 1968; Pecce and Fabbrocino 1999; Debernardi and Taliano 2002; Haskett *et al*. 2009) and HSC beams (Pecce and Fabbrocino 1999; Ko *et al*. 2001; Lopes and Bernardo 2003) by other researchers during static beam tests as well as those predicted by Eurocode 2 (EC2 2004) based on UK National Annex. The comparisons of NSC and HSC beams are summarised in Tables 4 and 5 respectively. The length of plastic hinge from the point of maximum moment in the beam is taken as the lower bound value of 0.4d obtained by Mendis (2001), where d is the effective depth. From the tables, it is evident that the rotation capacities evaluated by Eq. (6) are closer to the measured rotation and the differences are mostly within 30%. When compared with the rotation capacities predicted by the Eurocode 2, Eq. (6) has the average predicted rotation capacities closer to the measured values and smaller

standard deviation. It is also seen from the tables that the rotation capacities of concrete beams predicted by Eurocode 2 are too conservative. Moreover, the overestimation increases as the concrete strength increases.

4. Deformability design of concrete beams

In the design of NSC and HSC beams, both strength and deformability needs to be considered. This is because the provision of adequate strength and deformability will provide extra safety to the structures under sudden impact or blasting, and extreme events like earthquake attack. However, the design of beam for a prescribed pair of flexural strength and deformability requirement is not straightforward since the major factors affecting the deformability of concrete beams, which are the concrete strength, degree of reinforcement, steel yield strength, steel ratio and confining pressure, will also affect the flexural strength. Therefore, the design process may become iterative. To avoid such an iterative design process, a more systematic way of simultaneous design of both flexural strength and deformability of concrete beams is proposed. A series of design charts will be derived for this purpose. In regard of singly-reinforced concrete beams, a simplified method of evaluating the range of required tension steel to satisfy the prescribed strength and deformability required is developed.

4.1 Design charts

It is understood that the concrete strength, areas and yield strength of tension and compression steel, and confining steel are the major factors affecting the strength and deformability of NSC and HSC beams. To assess how these parameters influence the strength and deformability, the variation of deformability against flexural strength for concrete beams with different concrete strength, compression steel ratio and confining pressure are plotted in Figs 7 to 9 respectively. In each of the figures, the plotted curves represent the maximum limit of flexural strength and deformability that can be achieved simultaneously by the beam. These graphs can be adopted for design of concrete beams for a pair of given strength and deformability requirement in a single step. The major advantage of this method is that it will provide different feasible design options, such as

using HSC and/or HSS, adding compression and/or confining steel in order to improve the strength-and-deformability performance. The final design option can be decided by taking into account the economical factors, architectural and sustainability requirements.

To use the proposed design charts, it is advocated from economical point of view to adopt Fig 7 in the first place, where no compression and confining steel is needed. If there is no valid design solution even after adopting the highest concrete strength of f_{co} = 100 MPa, some compression steel (Fig 8) and confining steel (Fig 9) can be added to improve the strength-and-deformability performance. If it is decided that compression steel is needed, the required compression steel ratio can be determined by using successively ρ_c = 0.5%, ρ_c = 1.0%, ρ_c = 1.5% and ρ_c = 2.0% for a particular concrete strength until the prescribed requirement is satisfied. If the flexural strength and deformability requirements could not be met even when a compression steel ratio of 2.0% and f_{co} = 100 MPa are used, then there is no other option apart from increasing the size of the beam. The use of compression steel greater than 2.0% is generally not recommended (EC2 2004).

If the addition of confining steel is preferred other than adding compression steel to avoid steel congestion in the proximity of the beam-column joint, Fig 9 can be adopted. Similar to Fig 9, the required amount of confining steel can be determined by using successively f_r = 1.0, 2.0, 3.0 and 4.0 MPa from the lowest concrete strength of f_{co} = 40 MPa. If the flexural strength and deformability requirements could not be satisfied even when f_{co} = 100 MPa and f_r = 4.0 MPa are used, then there is no other option apart from increasing the size of the beam section. The use of $f_r > 4.0$ MPa is not recommended because the confining steel will be too congested around the plastic hinge region that causes severe steel congestion in the proximity of beam-column joints.

4.2 Design inequalities for singly-reinforced concrete beams

In the design of secondary beams, which are supported by the primary beams, the depth of beam is usually not critical and the provision of singly-reinforced concrete beams tends to be sufficient to satisfy both the flexural strength and deformability

requirements. In this circumstance, a simplified design method based on the proposed equation (Eq. 5) can be used without going through the design charts. The idea of this design method is to firstly determine the upper bound value of the tension steel ratio that would satisfy the given deformability requirement. After that, the lower bound value of the tension steel ratio will be determined from the given flexural strength requirement. The final design option can be taken as any tension steel ratio within the calculated range by considering other factors such as cost and architectural requirement. In the event that there are no critical factors restricting the selection of the tension steel ratio, it is recommended to design the beam with the median value because it will provide both strength and deformability slightly more than adequate. The provision of the upper bound value of tension steel ratio is not recommended because: (1) it will provide excessive flexural strength to the beam that violates the "strong column - weak beam" design philosophy or increase the risk of having brittle shear failure. (2) The provision of a more than sufficient flexural deformability is always beneficial to the structures.

Generally in the design of concrete beams, the strength of concrete is prescribed. Therefore, Eq. (6) can be used to check whether a particular minimum requirement of deformability is satisfied by a beam section of certain concrete strength. Suppose the deformability requirement for design is $\theta_{pl,d}$, the maximum limit of λ for a singly-reinforced beam section can be calculated by the following inequalities:

$$\theta_{pl,d} \le 0.03(f_{co})^{-0.3}(\lambda)^{-1.0}\left(\frac{f_{yt}}{460}\right)^{0.3} \tag{7a}$$

$$\lambda \le 0.03(\theta_{pl,d})^{-1.0}\left(\frac{f_{yt}/460}{f_{co}}\right)^{0.3} \tag{7b}$$

The minimum tension steel ratio is determined by the flexural strength requirement (M_d). Using the equivalent rectangular concrete stress block stipulated in Eurocode 2 (EC2 2004) and take $f_{co} = \alpha f_c'$, the minimum limit of $\lambda = \rho_t/\rho_{bo}$ can be calculated by the following inequalities:

$$\lambda \geq \frac{-f_{co} + f_{co}\sqrt{1+\left(\frac{2}{f_{co}}\right)\left(\frac{M_d}{bd^2}\right)}}{f_{yt}\rho_{bo}} \tag{8}$$

Combining Inequalities (7b) and (8), the suitable range of λ for designing a beam section without compression and confining steel with prescribed concrete strength f_{co} can be derived for a pair of deformability $\theta_{pl,d}$ and strength requirements M_d/bd^2:

$$\frac{-f_{co} + f_{co}\sqrt{1+\left(\frac{2}{f_{co}}\right)\left(\frac{M_d}{bd^2}\right)}}{f_{yt}\rho_{bo}} \leq \lambda \leq 0.03(\theta_{pl,d})^{-1.0}\left(\frac{f_{yt}/460}{f_{co}}\right)^{0.3} \tag{9}$$

5. Application and numerical examples

5.1 Deformability design for structures in non-seismic regions

In the deformability design of concrete beams in non-seismic region, the rotational capacity demand is usually not critical and the objective for designing deformability is to provide extra safety to the structures under accidental impact and overloading. The normalised rotation capacity required can be derived from the deemed-to-comply reinforcement detailing rules currently stipulated in the Eurocode (EC2 2004). In Eurocode 2, it has been specified in Clause 5.6.3.2 that the neutral axis depth of concrete beam should not be more than $0.45d$ when $f_{ck} \leq 50$ MPa or $0.35d$ when $f_{ck} > 50$ MPa, in which f_{ck} is the characteristic concrete cylinder strength and d is the effective depth. This will imply a range of deformability to be provided for beam sections with different concrete strength. For a more conservative approach, the deformability provided to a beam section with $f_{ck} = 30$ MPa (which is about the lowest concrete strength used nowadays) and $f_{yt} = 400$ MPa (minimum steel yield strength allowed by the Eurocode 2) is adopted. To work out the required deformability, it is noted that limiting the neutral axis depth to $0.45d$ for beam section of $f_{ck} = 30$ MPa and $f_{yt} = 400$ MPa is equivalent of limiting the maximum value of λ to 0.71, assuming an

ultimate concrete strain of 0.0035 and elastic modulus of steel of 200 kN/mm^2. The resulting deformability can be calculated using Eq. (6). Substituting $f_{co} = 0.85f_{ck} = 25.5$ MPa, $f_{yt} = 400$ MPa and $\lambda = 0.71$ into Eq. (6), it is evaluated that $\theta_{pl,d} = 0.015$ rad, which is the proposed deformability for designing concrete beams in non-seismic regions.

As an example, suppose the given flexural strength requirement is $M_d/bd^2 = 10.0$, the appropriate design option for a concrete beam section with $f_{co} = 60$ MPa and $f_{yt} = 600$ MPa located in non-seismic regions ($\theta_{pl,d} = 0.015$ rad) can be obtained from:

(1) Providing just sufficient strength but generous deformability:

Fig 7(a); $\lambda = 0.50$; $\rho_c = 0\%$; $M_p/bd^2 = 10.0$; $\theta_{pl,d} = 0.017$ rad.

Or Fig 7(b); $\rho_t = 1.8\%$; $\rho_c = 0\%$; $M_p/bd^2 = 10.0$; $\theta_{pl,d} = 0.017$ rad.

(2) Providing just sufficient deformability but generous strength:

Fig 7(a); $\lambda = 0.59$; $\rho_c = 0\%$; $M_p/bd^2 = 11.0$; $\theta_{pl,d} = 0.015$ rad.

Or Fig 7(b); $\rho_t = 2.1\%$; $\rho_c = 0\%$; $M_p/bd^2 = 11.0$; $\theta_{pl,d} = 0.015$ rad.

Some compression steel can be added to reduce beam size. For example, say $M_d/bd^2 = 18.0$ for a 25% reduction in beam depth.

(3) Fig 8(b); $\lambda = 0.65$; $\rho_c = 1.0\%$; $M_p/bd^2 = 18.0$; $\theta_{pl,d} = 0.015$ rad.

Alternatively, if the overall beam depth is not critical, the allowable range of λ can be determined by Inequality (9). Based on the deformability requirement $\theta_{pl,d} = 0.015$ rad, the permissible range of λ can be calculated by:

$$\lambda \le 0.03(\theta_{pl,d})^{-1.0}\left(\frac{f_{yt}/460}{f_{co}}\right)^{0.3} = \frac{0.03}{0.015}\times\left(\frac{600/460}{60}\right)^{0.3} = 0.63$$

Based on the strength requirement $M_d/bd^2 = 10.0$, the permissible range of λ can be calculated by:

$$\lambda \ge \frac{-f_{co} + f_{co}\sqrt{1+\left(\frac{2}{f_{co}}\right)\left(\frac{M_d}{bd^2}\right)}}{f_{yt}\rho_{bo}} = \frac{-60+60\sqrt{1+\left(\frac{2}{60}\right)\times 10}}{600\times 0.0369} = 0.42$$

Therefore, the permissible range of λ is $0.42 \le \lambda \le 0.63$. Select the median value of λ (= 0.53) to provide flexural strength and deformability slightly larger than required, the design tension steel ratio is given by $\rho_t = \lambda \times \rho_{bo} = 0.53 \times 3.69\% = 2.0\%$.

5.2 Deformability design for structural in low-moderate seismicity regions

The major objective of deformability design of concrete beams in low to moderate seismicity region is to allow sufficient rotation capacity of concrete beam to deform with plastic hinges formation such that moment redistribution can be carried out. As per Clause 5.6.2(1) of Eurocode 2 (EC2 2004), this can be achieved by plastic analysis that ensures adequate ductility and rotation capacities of the critical sections for the envisage mechanism to be formed without the need of performing any direct check. The deemed-to-comply rules for plastic analysis specified in the Eurocode 2 are to restrict further the neutral axis depth in beams/slabs to $0.25d$ for concrete not more than 50 MPa and $0.15d$ for concrete grade more than 50 MPa. Similar to the non-seismic design, the recommended deformability for beams in low to moderate seismicity regions, is taken as that of the beam sections with f_{ck} = 30 and f_{yt} = 400 MPa. To work out the required deformability, it is noted that limiting the neutral axis depth to $0.25d$ for beam section of f_{ck} = 30 MPa and f_{yt} = 400 MPa is equivalent of limiting the maximum value of λ to 0.39, assuming an ultimate concrete strain of 0.0035 and elastic modulus of steel of 200 kN/mm^2. The resulting deformability can be calculated using Eq. (6). Substituting $f_{co} = 0.85f_{ck}$ = 25.5 MPa, f_{yt} = 400 MPa and λ = 0.39 into Eq. (6), it is evaluated that $\theta_{pl,d}$ = 0.03 rad.

As an example, suppose the given flexural strength requirement is M_d/bd^2 = 6.0, the appropriate design option for a concrete beam section with f_{co} = 60 MPa and f_{yt} = 600 MPa and located in non-seismic regions ($\theta_{pl,d}$ = 0.030 rad) can be obtained from:

(1) Providing just sufficient strength but generous deformability:

Fig 7(a); λ = 0.3; ρ_c = 0%; M_p/bd^2 = 6.0; $\theta_{pl,d}$ = 0.032 rad.

Or Fig 7(b); ρ_t = 1.1%; ρ_c = 0%; M_p/bd^2 = 6.0; $\theta_{pl,d}$ = 0.032 rad.

(2) Providing just sufficient deformability but generous strength:

Fig 7(a); λ = 0.35; ρ_c = 0%; M_p/bd^2 = 6.5; $\theta_{pl,d}$ = 0.03 rad.

Or Fig 7(b); ρ_t =1.3%; ρ_c = 0%; M_p/bd^2 = 6.5; $\theta_{pl,d}$ = 0.03 rad.

Some compression steel can be added to reduce beam size. For example, say M_d/bd^2 = 11.0 for a 25% reduction in beam depth.

(3) Fig 8(b); λ = 0.35; ρ_c = 0.7%; ρ_t = 2.0%; M_p/bd^2 = 11.0; $\theta_{pl,d}$ = 0.03 rad.

Alternatively, for singly-reinforced beam section, the allowable range of λ can be determined by Inequality (9). Based on the deformability requirement $\theta_{pl,d}$ = 0.03 rad, the permissible range of λ can be calculated by:

$$\lambda \le 0.03(\theta_{pl,d})^{-1.0}\left(\frac{f_{yt}/460}{f_{co}}\right)^{0.3} = \frac{0.03}{0.03}\times\left(\frac{600/460}{60}\right)^{0.3} = 0.32$$

Based on the strength requirement M_d/bd^2 = 11.0, the permissible range of λ can be calculated by:

$$\lambda \ge \frac{-f_{co}+f_{co}\sqrt{1+\left(\frac{2}{f_{co}}\right)\left(\frac{M_d}{bd^2}\right)}}{f_{yt}\rho_{bo}} = \frac{-60+60\sqrt{1+\left(\frac{2}{60}\right)\times 6}}{600\times 0.0369} = 0.26$$

Therefore, the permissible range of λ is $0.26 \le \lambda \le 0.32$. Select the median value of λ (= 0.29) to provide flexural strength and deformability slightly larger than required, the design tension steel ratio is given by $\rho_t = \lambda \times \rho_{bo} = 0.29 \times 3.69\% \approx 1.1\%$.

6. Conclusions

This paper studied the major factors affecting the deformability of NSC and HSC beams using nonlinear moment-curvature analysis. The deformability is expressed in terms of normalised rotation capacity. The actual rotation capacity of the beam sections can be obtained by multiplying the normalised rotation capacity with the plastic hinge length. From the results, it was evident that the critical factors that affect the deformability of concrete beams are the degree of reinforcement λ, concrete strength

and confining pressure. The deformability decreases as λ increases until reaching 1.0. After that, the deformability remains relatively constant with λ. On the other hand, the effects of concrete strength on deformability of concrete beams are dependent other factors. At a fixed λ, the deformability decreases as the concrete strength increases; whereas at a fixed tension steel ratio, the deformability increases as the concrete strength increases. Lastly, the deformability of concrete beams always increases as the confining pressure increases.

Apart from deformability, the above critical factors will also affect the flexural strength at the same time. Therefore, the design of concrete beams to satisfy a pair of flexural strength and deformability requirement will become an iterative process. This is because the above factors (excluding confining pressure) will have opposite effects on flexural strength and deformability. To resolve the problem, the author has developed a method of designing the flexural strength and deformability of concrete beams simultaneously. Two methods were proposed. The first method based on developing a series of design charts plotting deformability against flexural strength for various combinations of concrete strength, degree of reinforcement, steel yield strength and confining pressure. The appropriate design option can be looked up from these design charts taking into account other engineering factors. For beam sections that do not require the provision of compression and confining steel, an alternative method of calculating the range of λ using flexural strength and deformability requirement is developed.

As applications of the proposed design methods, two numerical examples were given for designing concrete beams in non-seismic regions and in regions of low to moderate seismicity with prescribed strength and deformability requirements. The deformability requirement for theses regions is calculated based on the deemed-to-comply rules currently stipulated in Eurocode 2, which are 0.015 and 0.03 rad respectively.

Acknowledgement

Support from Seed Funding Programme for Basic Research (Project Code: 200910159034) provided by The University of Hong Kong is gratefully acknowledged.

References

1. Attard M.M. and Setunge S. (1996), "The stress strain relationship of confined and unconfined concrete", *ACI Materials Journal*, **93**(5), 432-442.
2. Au F.T.K., Chan K.H.E., Kwan A.K.H. and Du J.S. (2009), "Flexural ductility of prestressed concrete beams with unbonded tendons", *Computers and Concrete*, **6**(6), 451-472.
3. Bai Z.Z. and Au F.T.K. (2009) "Effects of strain hardening of reinforcement on flexural strength and ductility of reinforced concrete columns", *The Structural Design of Tall and Special Buildings*, doi:10.1002/tal.554.
4. Bilodeau A. and Malhotra V.M. (2000), "High-volume fly-ash system: Concrete solution for sustainable development", *ACI Materials Journal*, **97**, 41-48.
5. Chen X.W. and Han Z.L. (2010), "Research summary on long-span connected tall building structure with viscous dampers", *The Structural Design of Tall and Special Buildings*, **19**(4), 439-456.
6. Choi S., Lee S., Hong S. and Kim J. (2008), "Structural capacities of tension side for CFT square column-to-bean connections with combined-cross diaphragm", *Advances in Structural Engineering*, **11**(2), 209-227.
7. Chung H.S., Moon B.W., Lee S.K., Park J.H. and Min K.W. (2009), "Seismic performance of friction dampers using flexure of RC shear wall system", *The Structural Design of Tall and Special Buildings*, **18**, 807-822.
8. Debernardi P.G. and Taliano M. (2002), "On evaluation of rotation capacity of reinforced concrete beams", *ACI Structural Journal*, **99**(3), 360-368.
9. EC 2 (2004), Eurocode 2: *Design of concrete structures: Part 1-1: General rules and rules for buildings*, UK, 225pp.
10. Ellobody E. and Young B. (2006), "Design and behaviour of concrete-filled cold-formed stainless steel tube columns", *Engineering Structures*, **28**, 716-728.
11. Englekirk R.E. (2008), "A call for change in seismic design procedures", *The Structural Design of Tall and Special Buildings*, **17**, 1005-1013.

12. Feng R. and Young B. (2009) "Behaviour of Concrete-filled Stainless Steel Tubular X-joints subjected to Compression", *Thin-walled Structures,* **47**(4), 365-374.
13. Feng R. and Young B. (2010), "Design of concrete-filled stainless steel tubular connections", *Advances in Structural Engineering*, **13**(3), 471-492.
14. Fry J.A., Hooper J.D. and Klemencic R. (2009), "Core wall case study design for Pacific Earthquake Engineering Research/California Seismic Safety Commission", *The Structural Design of Tall and Special Buildings*, **19**(1-2), 61-75.
15. Goel S.C., Liao W.C., Bayat M.R. and Chao S.H. (2009), "Performance-based plastic design (PBPD) method for earthquake-resistant structures: An overview", *The Structural Design of Tall and Special Buildings*, **19**(1-2), 115-137.
16. Gribniak, V.; Kaklauskas, G.; Bacinskas, D. (2008), "Shrinkage in reinforced concrete structures: A computational aspect", *Journal of Civil Engineering and Management,* **14**(1), 49–60.
17. Havaei G.R. and Keramati A. (2011) "Experimental and numerical evaluation of the strength and ductility of regular and cross spirally circular reinforced concrete columns for tall buildings under eccentric loading", *The Structural Design of Tall and Special Buildings*, **20**(2), 247-256.
18. Haskett M., Oehlers D.J., Mohamed Ali M.S. and Wu C. (2009), "Rigid body moment-rotation mechanism for reinforced concrete beam hinges", *Engineering Structures,* **31**, 1032-1041.
19. Heo J.S., Lee S.K., Park E., Lee S.H., Min K.W., Kim H., Jo J. and Cho B.H. (2009), "Performance test of a tuned liquid mass damper for reducing bidirectional responses of building structures", *The Structural Design of Tall and Special Buildings*, **18**, 789-805.
20. Ho J.C.M., Kwan A.K.H. and Pam H.J. (2003), "Theoretical Analysis of Post-peak Flexural Behaviour of Normal- and High-strength Concrete Beams", *The Structural Design of Tall and Special Buildings*, **12**(2), 109-125.
21. Ho J.C.M. and Pam H.J. (2003), "Inelastic design of low-axially loaded high-strength reinforced concrete columns", *Engineering Structures*, **25**(8), 1083-1096.
22. Ho J.C.M., Au F.T.K. and Kwan A.K.H. (2005), "Effects of strain hardening of steel reinforcement on flexural strength and ductility of concrete beams", *Structural Engineering and Mechanics*, **19**(2), 185-198.

23. Ho J.C.M., Lam J.Y.K. and Kwan A.K.H. (2010a), "Effectiveness of adding confinement for ductility improvement of high-strength concrete columns", *Engineering Structures*, **32**, 714-725.
24. Ho J.C.M. (2011), "Limited ductility design of reinforced concrete columns for tall buildings in low to moderate seismicity regions", *The Structural Design of Tall and Special Buildings*, **20**(1), 102-120.
25. Hong W.K., Park S.C., Kim H.C., Kim J.M., Kim S.I. and Lee S.G. (2010) "Experimental study of reinforced concrete beams strengthened with a GFRP channel and CFRP sheets", *The Structural Design of Tall and Special Buildings*, **19**(5), 497-517.
26. Jiang S.F., Wu Z.Q. and Niu D.S. (2010), "Experimental study on fire-exposed rectangular concrete-filled steel tubular (CFST) columns subjected to bi-axial force and bending", *Advances in Structural Engineering*, **13**(4), 551-560.
27. Kaklauskas, G.; Gribniak, V.; Bacinskas, D. Vainiūnas, P. (2009), "Shrinkage influence on tension stiffening in concrete members", *Engineering Structures,* **31**(6), 1305–1312.
28. Ko M.Y., Kim S.W. and Kim J.K. (2001), "Experimental study on the plastic rotation capacity of reinforced high strength concrete beams", *Materials and Structures*, **34**, 302-311.
29. Kwak H.G. and Kim S.P. (2010), "Simplified monotonic moment-curvature relation considering fixed-end rotation and axial force", *Engineering Structures*, **32**, 69-79.
30. Kwan A.K.H., Chau S.L. and Au F.T.K. (2006), "Improving flexural ductility of high-strength concrete beams", *Proceedings, Institution of Civil Engineers, Structures and Buildings*, **159**(4), 339-347.
31. Kwan A.K.H. and Wong H.H.C (2008), "Packing density of cementitious materials: Part 2-packing and flow of OPC+PFA+CSF", *Materials and Structures*, **41**, 773-784.
32. Lam L. and Teng J.G. (2009), "Stress-strain model for FRP-confined concrete under cyclic axial compression", *Engineering Structures*, **31**, 308-321.
33. Lam J.Y.K., Ho J.C.M. and Kwan A.K.H. (2009), "Flexural ductility of high-strength concrete columns with minimal confinement", *Materials and Structures*, **42**(7), 909-921.

34. Lee S.K., Lee. S.Y., Min K.W., Moon B.W., Youn K.J. and Hwang J.S. (2009), "Performance evaluation of an MR damper in building structures considering soil-structure interaction effects", *The Structural Design of Tall and Special Buildings*, **18**, 105-115.
35. Lam S.S.E., Wu B., Liu Z.Q. and Wong Y.L. (2008), "Experimental study on seismic performance of coupling beams not designed for ductility", *Structural Engineering and Mechanics*, **28**(3), 317-333.
36. Lopes S.M.R. and Bernardo L.F.A. (2003), "Plastic rotation capacity of high-strength concrete beams", *Materials and Structures*, **36**, 22-31.
37. Lu Y. (2009), "Modelling of concrete structures subjected to shock and blast loading: An overview and some recent studies", *Structural Engineering and Mechanics*, **32**(2), 235-249.
38. Mander J.B., Priestley M.J.N. and Park R. (1988), "Theoretical stress-strain model for confined concrete", *Journal of Structural Engineering, ASCE*, **114**(8), 1804-1825.
39. Marano G.C. and Greco R. (2009), "Robust optimum design of tuned mass dampers for high-rise buildings under moderate earthquakes", *The Structural Design of Tall and Special Buildings*, **18**, 823-838.
40. Mendis P. (2001), "Plastic hinge lengths of normal and high-strength concrete in flexure", *Advances in Structural Engineering*, **4**(4), 189-195.
41. Nam J.W., Kim H.J., Yi N.H., Kim I.S., Kim J.J.H. and Choi H.J. (2009), "Blast analysis of concrete arch structures for FRP retrofitting design", *Computers and Concrete*, **6**(4), 305-318.
42. Nawy E.G., Danesi R.F. and Grosko J.J. (1968), "Rectangular spiral binders effect on plastic hinge rotation capacity in reinforced concrete beams", *ACI Journal*, **65**(12), 1001-1010.
43. NZS 3101, Standards New Zealand (2006), *Concrete Structures Standard, Part 1 - The Design of Concrete Structures*, Wellington, New Zealand.
44. Pam H.J., Kwan A.K.H. and Ho J.C.M. (2001), "Post-peak behavior and flexural ductility of doubly reinforced normal- and high-strength concrete beams", *Structural Engineering and Mechanics*, **12**(5), 459-474.

45. Pam H.J. and Ho J.C.M. (2009), "Length of critical region for confinement steel in limited ductility high-strength reinforced concrete columns", *Engineering Structures*, **31,** 2896-2908.
46. Park R. and Ruitong D. (1988), "Ductility of doubly reinforced concrete beam sections", *ACI Structural Journal*, **85**(2), 217-225.
47. Park S., Choi S., Park Y., Kim Y. and Kim J. (2008), "Ductility characteristics of partially restrained beam-to-column composite connections in concrete filled square tubes", *Advances in Structural Engineering*, **11**(5), 565-575.
48. Pecce M. and Fabbrocino G. (1999), "Plastic rotation capacity of beams in normal and high-performance concrete", *ACI Structural Journal*, **96**(2), 290-296.
49. Restrepo J.I., Seible F., Stephan B. and Schoettler M.J. (2006), "Seismic testing of bridge columns incorporating high-performance materials", *ACI Structural Journal*, **103**(4), 496-504.
50. Ribakov Y. (2009), "Base-isolated structures with selective controlled semi-active friction dampers", *The Structural Design of Tall and Special Buildings*, http://dx.doi.org/10.1002/tal.527
51. Sabouri-Ghomi S., Kharrazi M.H.K., Mam-Azizi S.D. and Sajadi R.A. (2008) "Buckling behavior improvement of steel plate shear wall systems", *The Structural Design of Tall and Special Buildings*, **17**, 823-837.
52. Scrivener K.L. and Kirkpatrick R.J. (2008), "Innovation in use and research on cementitious material", *Cement and Concrete Research*, **38**, 128-135.
53. Su R.K.L., Lam W.Y. and Pam H.J. (2009) "Experimental study of plate-reinforced composite deep coupling beams", *The Structural Design of Tall and Special Buildings*, **18**, 235-257.
54. Takewaki I. and Fujita K. (2009), "Earthquake input energy to tall and base-isolated buildings in time and frequency dual domains", *The Structural Design of Tall and Special Buildings*, **18**, 589-606.
55. Tsang H.H., Su R.K.L., Lam N.T.K. and Lo S.H. (2009), "Rapid assessment of seismic demand in existing building structures", *The Structural Design of Tall and Special Buildings*, **18**, 427-439.
56. Weerheijm J., Mediavilla J. and van Doormaal J.C.A.M. (2009), "Explosive loading of multi storey RC buildings: Dynamic response and progressive collapse", *Structural Engineering and Mechanics*, **32**(2), 193-212.

57. Wong H.H.C and Kwan A.K.H. (2008), "Packing density of cementitious materials: Part 1-measurement using a wet packing method", *Materials and Structures*, **41**, 689-701.
58. Wu Y.F., Oehlers D.J. and Griffith M.C. (2004), "Rational definition of the flexural deformation capacity of RC column sections", *Engineering Structures*, **26**, 641-650.
59. Wu Y.F. and Wei Y.Y. (2010), "Effects of cross-sectional aspect ratio on the strength of CFRP-confined rectangular concrete columns", *Engineering Structures*, **32**, 32-45.
60. Xu H., Provis J.L., Van Deventer J.S.J. and Krivenko P.V. (2008), "Characterization of aged slag concretes", *ACI Materials Journal*, **105**, 131-139.
61. Yamamoto K., Fujita K. and Takewaki I. (2009), "Instantaneous earthquake input energy and sensitivity in base-isolated building", *The Structural Design of Tall and Special Buildings*, http://dx.doi.org/10.1002/tal.539
62. Yan Z.H. and Au F.T.K. (2010) "Nonlinear dynamic analysis of frames with plastic hinges at arbitrary locations", *The Structural Design of Tall and Special Buildings*, **19**(7), 778-801.
63. Yousuf M. and Bagchi A. (2010), "Seismic performance of a 20-story steel-frame building in Canada", *The Structural Design of Tall and Special Buildings*, **19**(8), 901-921.
64. Zareian F., Krawinkler H., Ibarra L. and Lignos D. (2010), "Basic concepts and performance measures in prediction of collapse of buildings under earthquake ground motions", *The Structural Design of Tall and Special Buildings*, **19**, 167-181.
65. Zhou K.J.H., Ho J.C.M. and Su R.K.L. (2010), "Normalised rotation capacity for deformability evaluation of high-performance concrete beams", *Earthquakes and Structures*, **1**(3), 269-287.

List of Notations

A_{sb} Balanced steel area

A_{sc} Area of compression steel

A_{st} Area of tension steel

b	Breadth of beam section
d	Effective depth of beam section
d_b	Diameter of longitudinal steel
d_s	Diameter of confining steel
E_s	Elastic modulus of steel reinforcement
f_{co}	Peak stress on stress-strain curve of unconfined concrete
f_c'	Concrete cylinder strength
f_r	Confining pressure
f_y	Yield strength of steel reinforcement
f_{yc}	Yield strength of compression steel
f_{yt}	Yield strength of tension steel
h	Total depth of the beam section
ℓ_p	Plastic hinge length
M_d	Design value of moment capacity
M_p	Peak moment
α	Ratio of equivalent concrete stress to cylinder strength as stipulated in EC2
ε_{ps}	Residual plastic strain in steel reinforcement
ε_s	Strain in steel
θ_{pl}	Normalised rotation capacity of beam
$\theta_{pl,d}$	Design value of normalised rotation capacity
λ	Degree of reinforcement
ϕ_u	Ultimate curvature
ρ_b	Balanced steel ratio (= A_{sb}/bd)
ρ_{bo}	Balanced steel ratio for beam section with no compression steel
ρ_c	Compression steel ratio (= A_{sc}/bd)
ρ_t	Tension steel ratio (= A_{st}/bd)
σ_s	Stress in steel reinforcement

Tables

Table 1 Balanced steel ratios ρ_{bo} for tension steel yield strength f_{yt} = 400 MPa

f_{co} (MPa)	Balanced steel ratios without compression reinforcement ρ_{bo}(%)				
	f_r = 0 MPa	f_r = 1 MPa	f_r = 2 MPa	f_r = 3 MPa	f_r = 4 MPa
40	4.74	5.98	6.90	7.73	8.56
50	5.63	6.91	7.86	8.78	9.60
60	6.46	7.79	8.77	9.70	10.59
70	7.29	8.62	9.61	10.54	11.50
80	8.06	9.38	10.37	11.35	12.29
90	8.77	10.11	11.13	12.11	13.03
100	9.42	10.80	11.82	12.78	13.76

Table 2 Balanced steel ratios ρ_{bo} for tension steel yield strength f_{yt} = 600 MPa

f_{co} (MPa)	Balanced steel ratios without compression reinforcement ρ_{bo}(%)				
	f_r = 0 MPa	f_r = 1 MPa	f_r = 2 MPa	f_r = 3 MPa	f_r = 4 MPa
40	2.74	3.60	4.23	4.83	5.37
50	3.23	4.12	4.78	5.40	6.00
60	3.69	4.61	5.29	5.93	6.55
70	4.13	5.06	5.76	6.41	7.04
80	4.56	5.50	6.19	6.85	7.49
90	4.94	5.90	6.59	7.28	7.91
100	5.29	6.27	6.97	7.67	8.29

Table 3 Balanced steel ratios ρ_{bo} for tension steel yield strength f_{yt} = 800 MPa

f_{co} (MPa)	Balanced steel ratios without compression reinforcement ρ_{bo}(%)				
	f_r = 0 MPa	f_r = 1 MPa	f_r = 2 MPa	f_r = 3 MPa	f_r = 4 MPa
40	1.82	2.48	2.96	3.42	3.84
50	2.13	2.82	3.33	3.80	4.25
60	2.43	3.14	3.66	4.14	4.61
70	2.70	3.43	3.96	4.45	4.93
80	2.97	3.69	4.22	4.75	5.21
90	3.22	3.95	4.50	5.00	5.49
100	3.44	4.19	4.74	5.22	5.74

Table 4 Comparison with experimental results on rotation capacities of NSC beams

Code	f_c' (MPa)	f_r (Mpa)	f_{yt} (Mpa)	ρ_t (%)	ρ_c (%)	θ_{pl} by Eq. (5) (rad) [1]	θ_{pl} by others (rad) [2]	θ_{pl} by EC2 (rad) [3]	[1]/[2]	[3]/[2]
Nawy *et al*. (1968)										
P9G1	33.6	0.00	328	1.73	0.71	0.0870	0.0650	0.0330	1.34	0.51
P11G3	35.1	0.50	328	1.73	0.71	0.1536	0.1110	0.0320	1.38	0.29
P3G4	37.5	1.30	452	1.73	0.71	0.1232	0.1340	0.0260	0.92	0.19
P4G5	39.1	1.30	452	1.73	0.71	0.1217	0.1360	0.0265	0.89	0.19
Pecce and Fabbocino (1999)										
A	41.3	0.98	471	2.60	0.05	0.0255	0.0220	0.0100	1.16	0.45
B	41.3	0.94	454	1.10	0.05	0.0736	0.1220	0.0265	0.60	0.22
Debernardi and Taliano (2002)										
T1A1	27.7	0.46	587	0.67	0.30	0.1433	0.1035	0.0310	1.38	0.30
T3A1	27.7	0.46	587	2.00	0.59	0.0270	0.0290	0.0080	0.93	0.28
T5A1	27.7	0.35	587	0.63	0.22	0.0978	0.1130	0.0300	0.87	0.27
T6A1	27.7	0.35	587	1.28	0.22	0.0311	0.0245	0.0160	1.27	0.65
Haskett *et al*. (2009)										
A1	38.2	0.67	315	1.47	0.0	0.0313	0.0360	0.0269	0.87	0.75
A2	42.3	0.32	318	1.47	0.0	0.0226	0.0205	0.0280	1.10	1.37
A3	41.0	0.31	336	1.47	0.0	0.0209	0.0168	0.0270	1.24	1.61
A4	42.9	1.29	315	2.95	0.0	0.0222	0.0305	0.0172	0.73	0.56
A5	39.6	0.59	314	2.95	0.0	0.0136	0.0207	0.0154	0.66	0.74
A6	41.1	0.31	328	2.95	0.0	0.0103	0.0118	0.0153	0.87	1.30
B1	43.0	0.65	329	1.47	0.0	0.0293	0.0277	0.0278	1.06	1.00
B2	41.8	0.31	322	1.47	0.0	0.0222	0.0152	0.0277	1.46	1.82
B3	42.9	1.29	321	2.95	0.0	0.0217	0.0218	0.0168	1.00	0.77
B4	42.9	0.64	323	2.95	0.0	0.0138	0.0120	0.0166	1.15	1.38
C2	26.0	0.39	329	1.47	0.0	0.0219	0.0258	0.0203	0.85	0.79
C3	25.6	0.32	330	1.47	0.0	0.0201	0.0187	0.0200	1.07	1.07
C4	25.9	1.23	325	2.95	0.0	0.0205	0.0297	0.0080	0.69	0.27
C5	23.4	0.64	328	2.95	0.0	0.0126	0.0130	0.0080	0.97	0.62
C6	27.4	0.34	319	2.95	0.0	0.0102	0.0125	0.0080	0.82	0.64
								Average	1.01	0.72
								Standard deviation	0.24	0.47

Table 5 Comparison with experimental results on rotation capacities of HSC beams

Code	f_c' (MPa)	f_r (Mpa)	f_{yt} (Mpa)	ρ_t (%)	ρ_c (%)	θ_{pl} by Eq. (5) (rad) [1]	θ_{pl} by others (rad) [2]	θ_{pl} by EC2 (rad) [3]	[1]/[2]	[3]/[2]
Pecce and Fabbocino (1999)										
AH	93.8	0.98	471	2.60	0.05	0.0271	0.0220	0.0170	1.23	0.77
CH	95.4	1.11	534	2.20	0.04	0.0300	0.0380	0.0170	0.79	0.45
Ko *et al*. (2001)										
6-65-1	66.6	2.26	415	3.59	0.79	0.0547	0.0472	0.0150	1.16	0.32
6-75-1	66.6	2.33	427	4.27	0.77	0.0399	0.0412	0.0100	0.97	0.24
8-50-1	82.1	2.42	443	3.35	0.80	0.0580	0.0482	0.0160	1.20	0.33
8-65-1	82.1	2.33	427	4.27	0.77	0.0398	0.0450	0.0100	0.88	0.22
8-75-1	82.1	2.15	394	4.97	0.79	0.0338	0.0484	0.0080	0.70	0.17
$7\text{-}62^{00}$-1	70.8	1.91	408	3.16	0.00	0.0403	0.0530	0.0135	0.76	0.25
$7\text{-}62^{15}$-1	70.8	1.91	408	3.16	0.79	0.0587	0.0510	0.0160	1.15	0.31
Lopes and Bernardo (2003)										
A(64.9-2.04)	64.9	0.59	555	2.04	0.20	0.0248	0.0200	0.0210	1.24	1.05
A(63.2-2.86)	63.2	0.62	575	2.86	0.20	0.0161	0.0180	0.0110	0.89	0.61
A(65.1-2.86)	65.1	0.62	575	2.86	0.20	0.0161	0.0150	0.0110	1.07	0.73
B(82.9-2.11)	82.9	0.59	555	2.11	0.20	0.0243	0.0210	0.0180	1.16	0.86
B(83.9-2.16)	83.9	0.59	555	2.16	0.20	0.0237	0.0200	0.0180	1.19	0.90
B(83.6-2.69)	83.6	0.62	575	2.69	0.20	0.0178	0.0210	0.0150	0.85	0.71
B(83.4-2.70)	83.4	0.62	575	2.70	0.20	0.0177	0.0200	0.0150	0.89	0.75
								Average	1.01	0.54
								Standard deviation	0.18	0.28

Figures

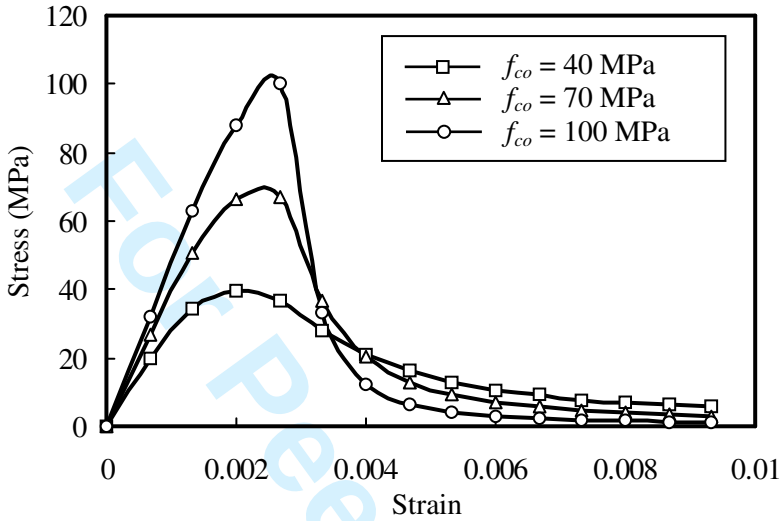

(a) Stress-strain curves of concrete

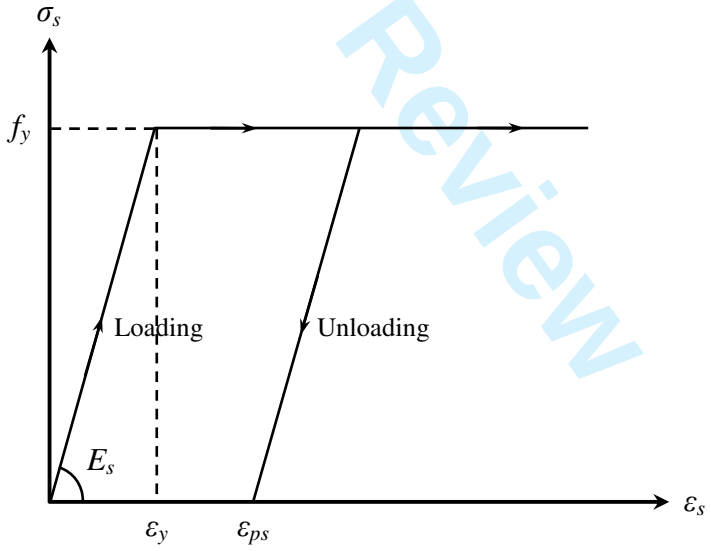

(b) Stress-strain curve of steel with stress-path dependence considered

Figure 1 Stress-strain curves of concrete and steel

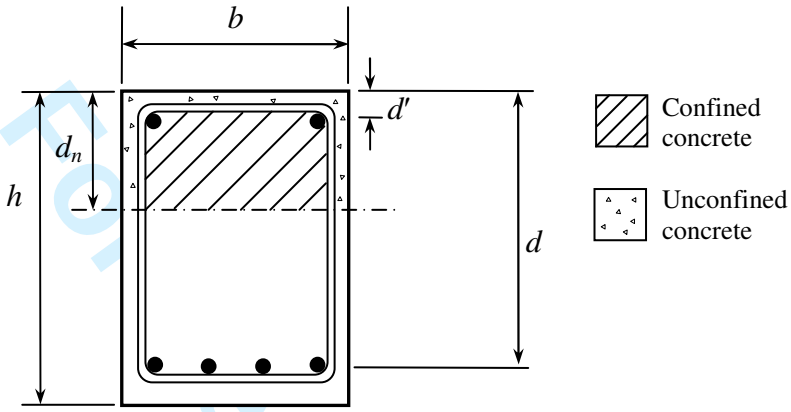

Section properties

- b = 300 mm
- h = 600 mm
- d' = 50 mm
- d = 550 mm
- f_{co} = 40 to 100 MPa
- f_y = 400 to 800 MPa
- f_r = 0 to 4 MPa
- $\rho_t = A_{st}/bd$ = 0.4 to $2\rho_b$
- $\rho_c = A_{sc}/bd$ = 0 to 2%

Figure 2 Beam sections analysed

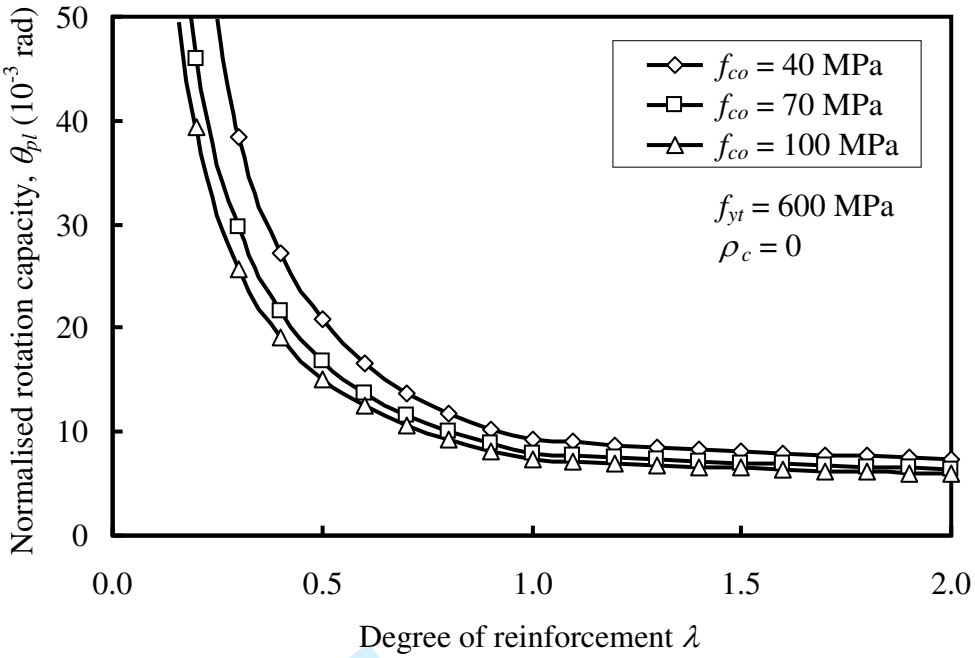

(a) θ_{pl} against λ

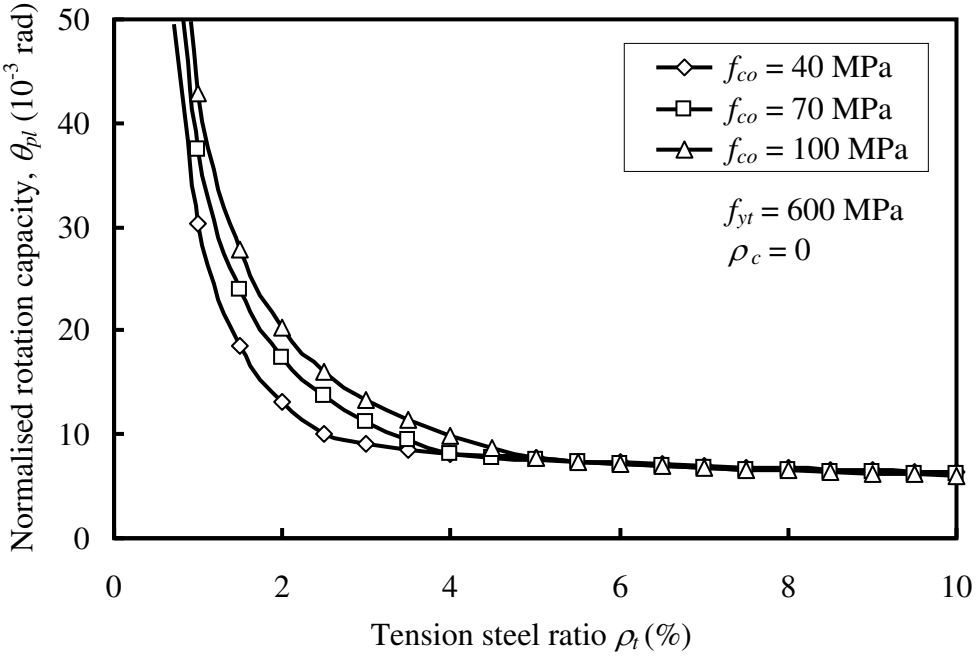

(b) θ_{pl} against ρ_t

Figure 3 Effects of concrete strength on deformability of concrete beams

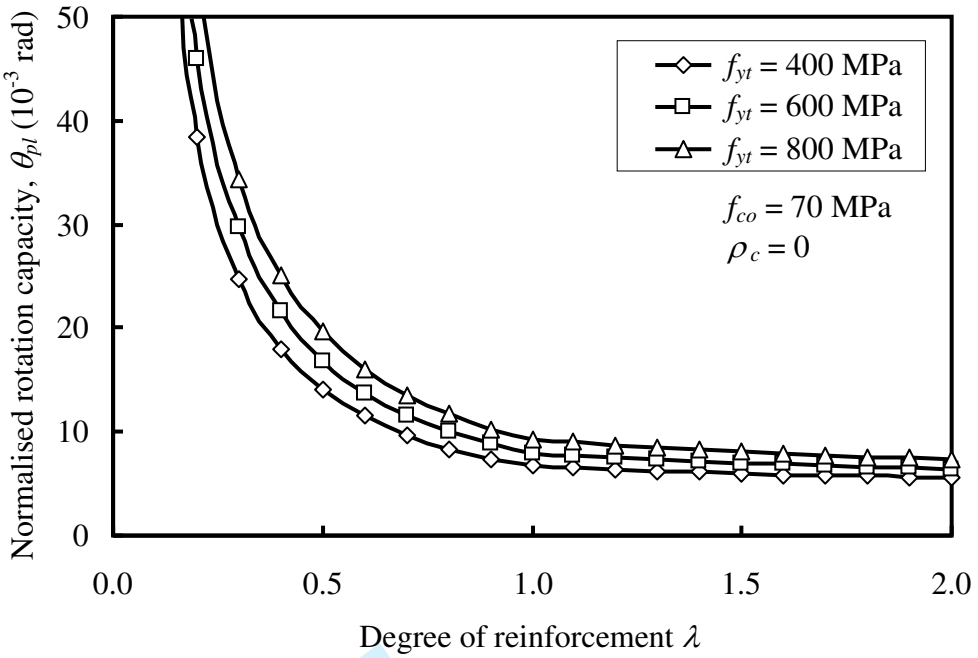

(a) θ_{pl} against λ

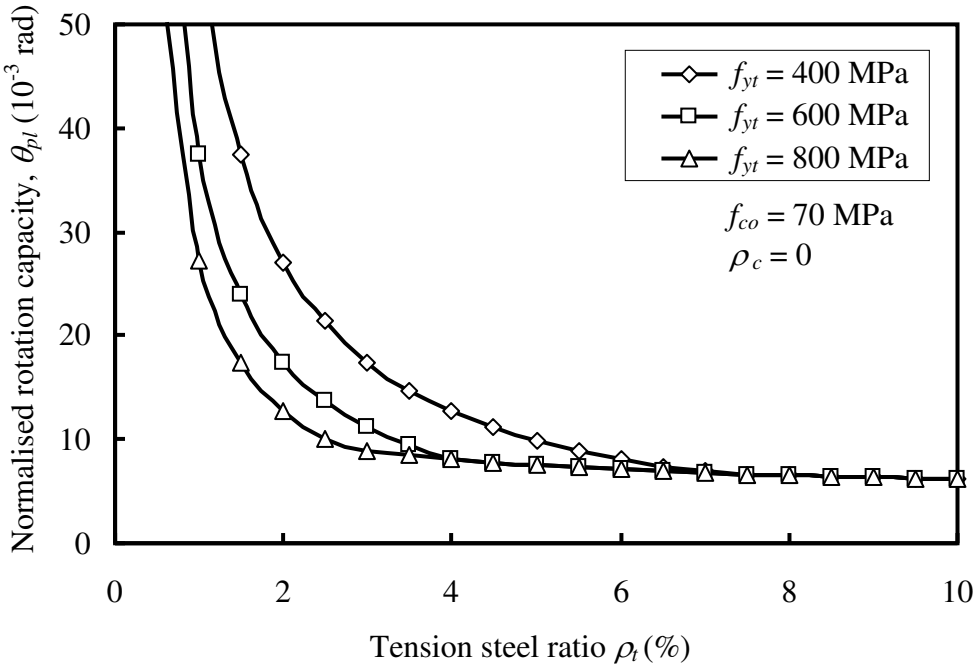

(b) θ_{pl} against ρ_t

Figure 4 Effects of tension steel yield strength on deformability of concrete beams

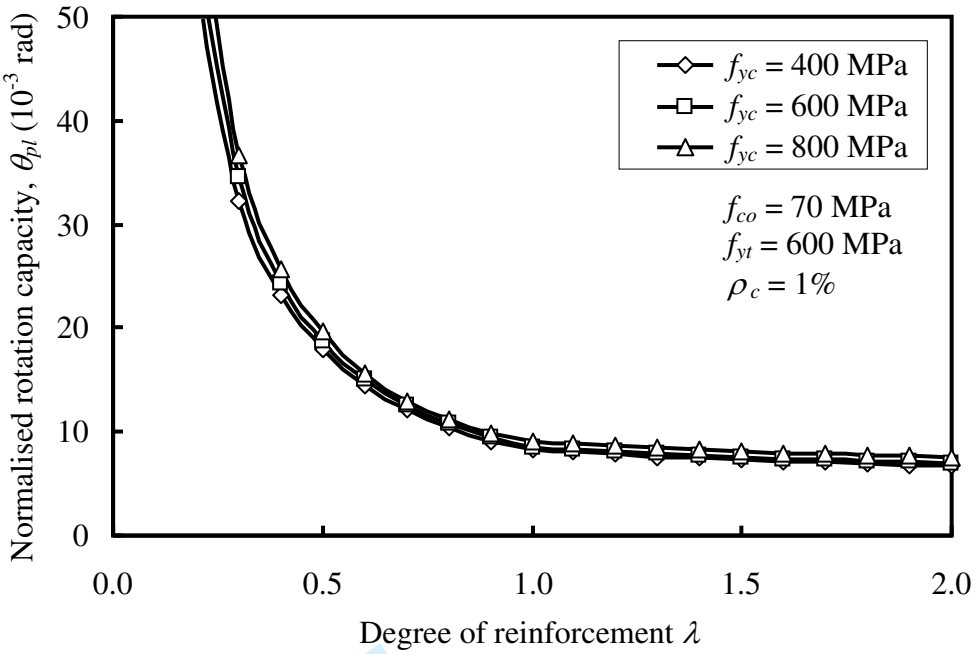

(a) θ_{pl} against λ

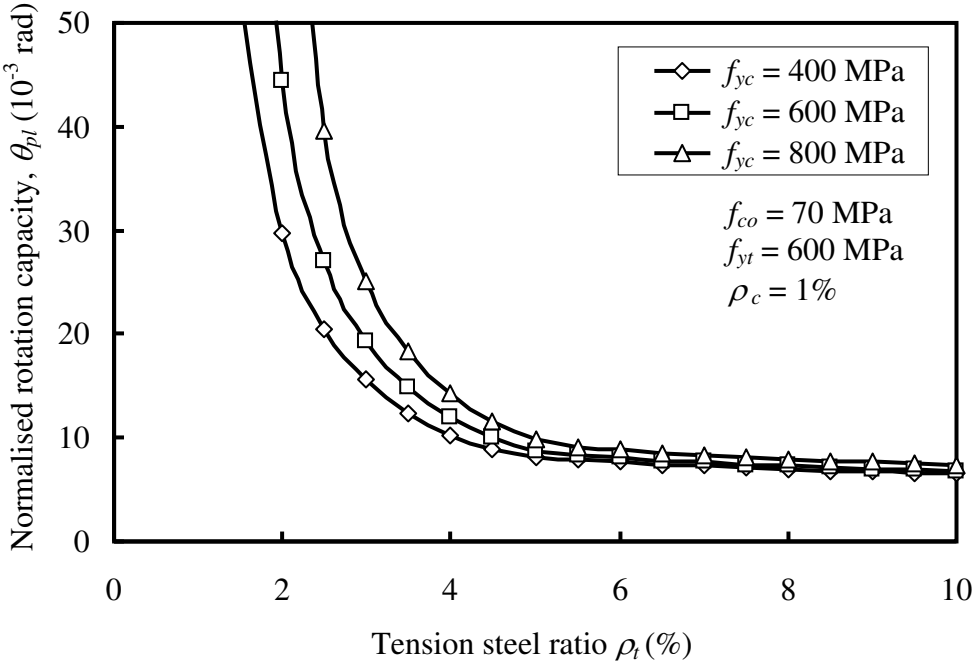

(b) θ_{pl} against ρ_t

Figure 5 Effects of compression steel yield strength on deformability of concrete beams

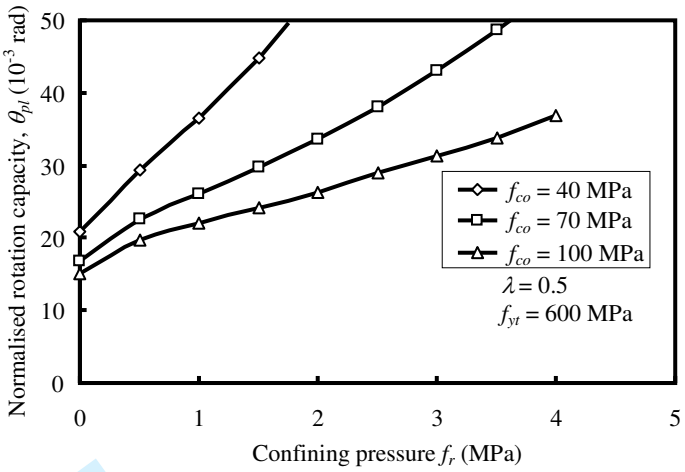

(a) θ_{pl} against f_r for different f_{co}

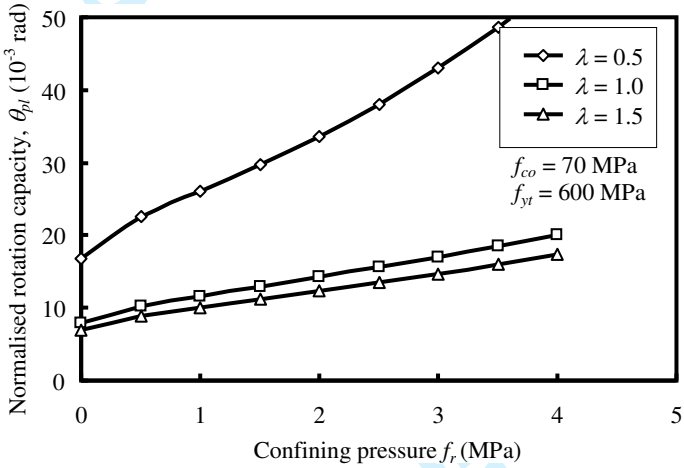

(b) θ_{pl} against f_r for different λ

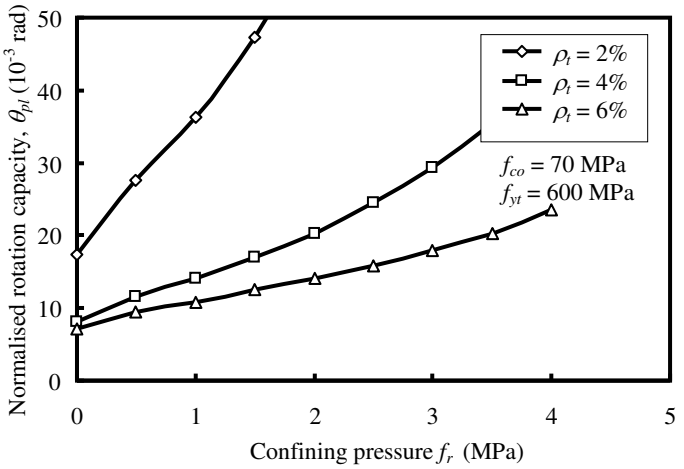

(c) θ_{pl} against f_r for different ρ_t

Figure 6 Effects of confining pressure on deformability of concrete beams

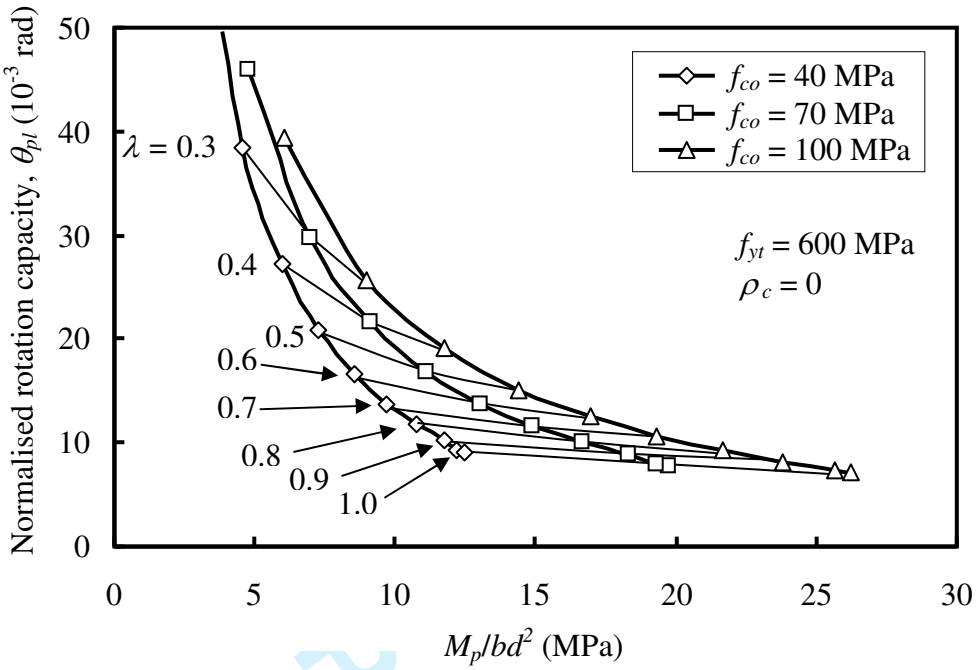

(a) For different levels of λ

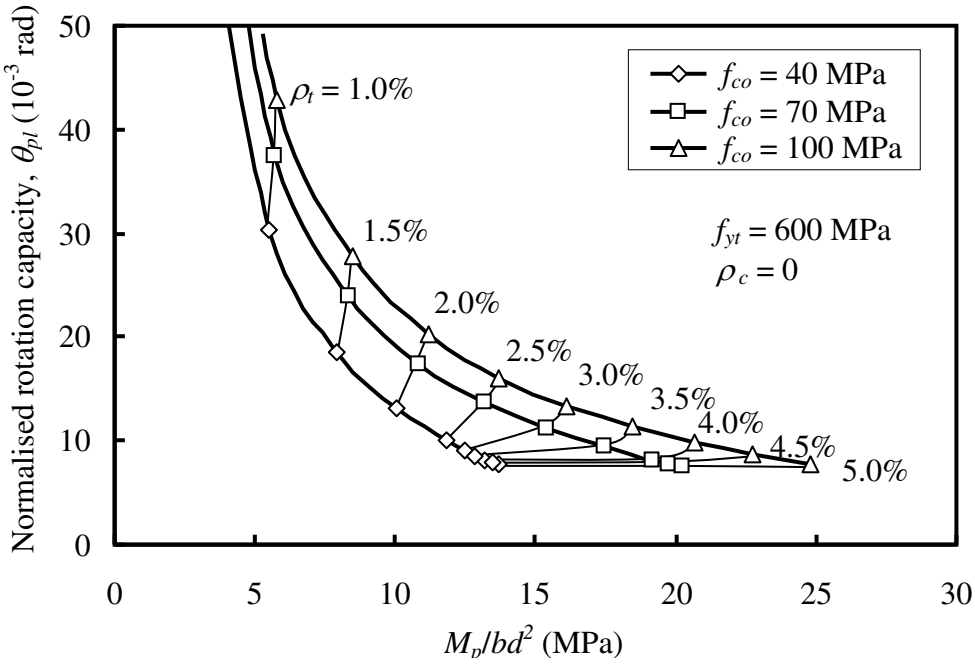

(b) For different levels of ρ_t

Figure 7 Design charts for beams with different concrete strength

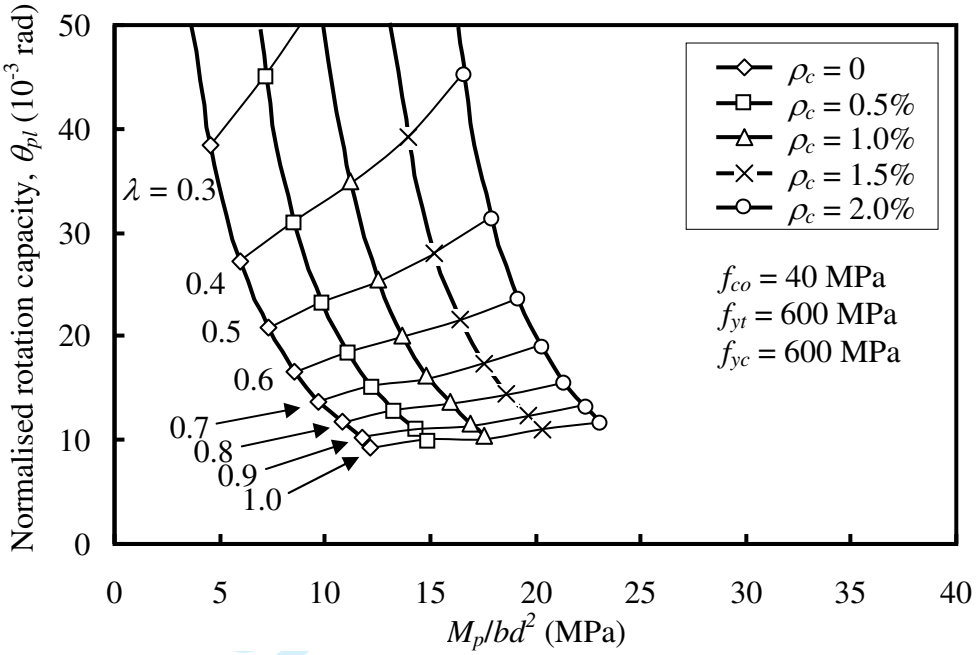

(a) f_{co} = 40 MPa, f_{yt} = f_{yc} = 600 MPa

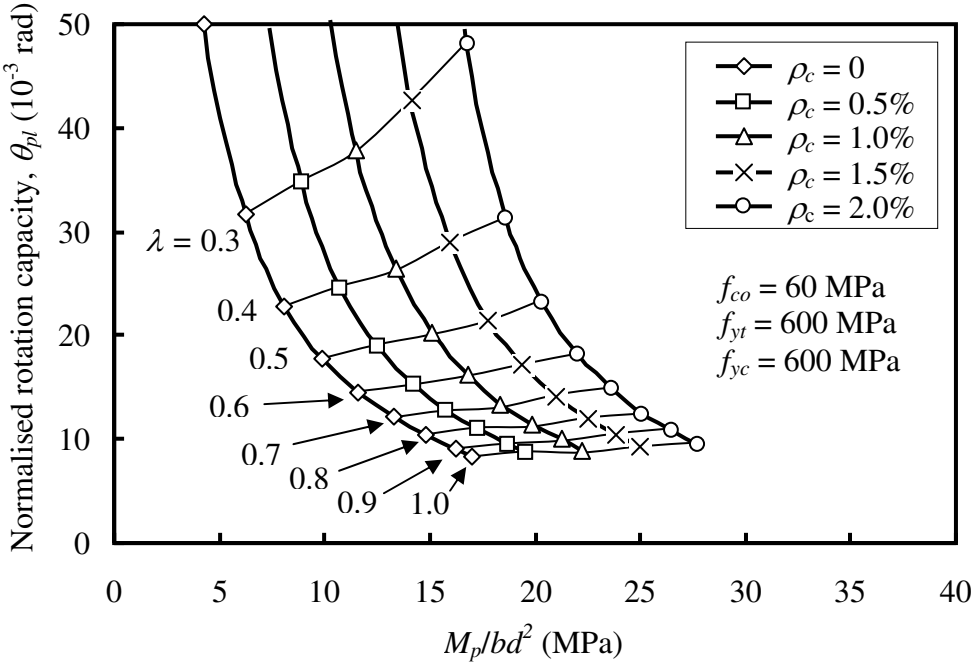

(b) f_{co} = 60 MPa, f_{yt} = f_{yc} = 600 MPa

Figure 8 Design charts for beams with different compression steel ratios

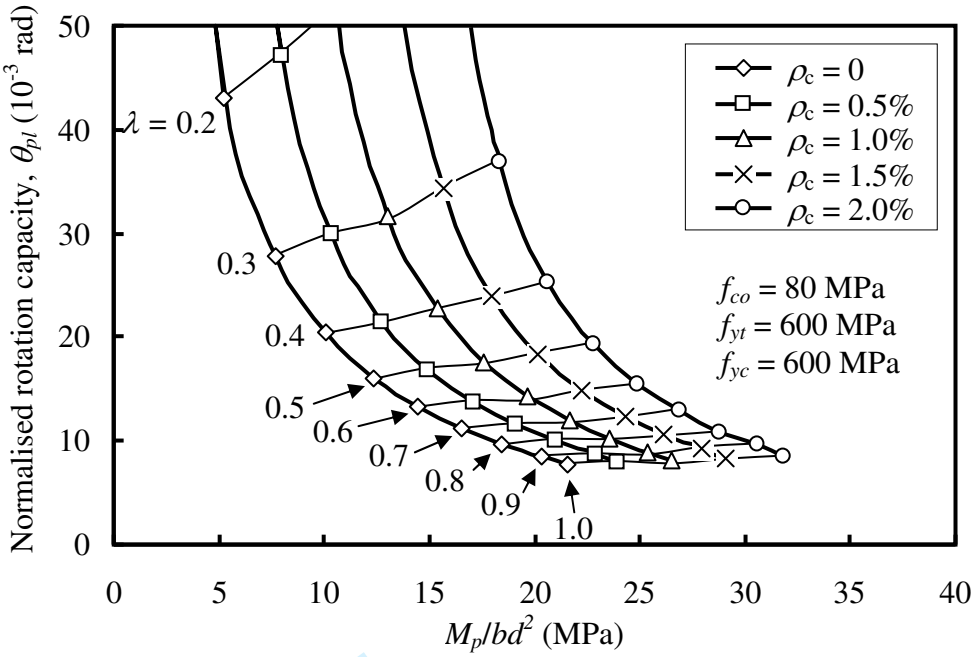

(c) f_{co} = 80 MPa, $f_{yt} = f_{yc}$ = 600 MPa

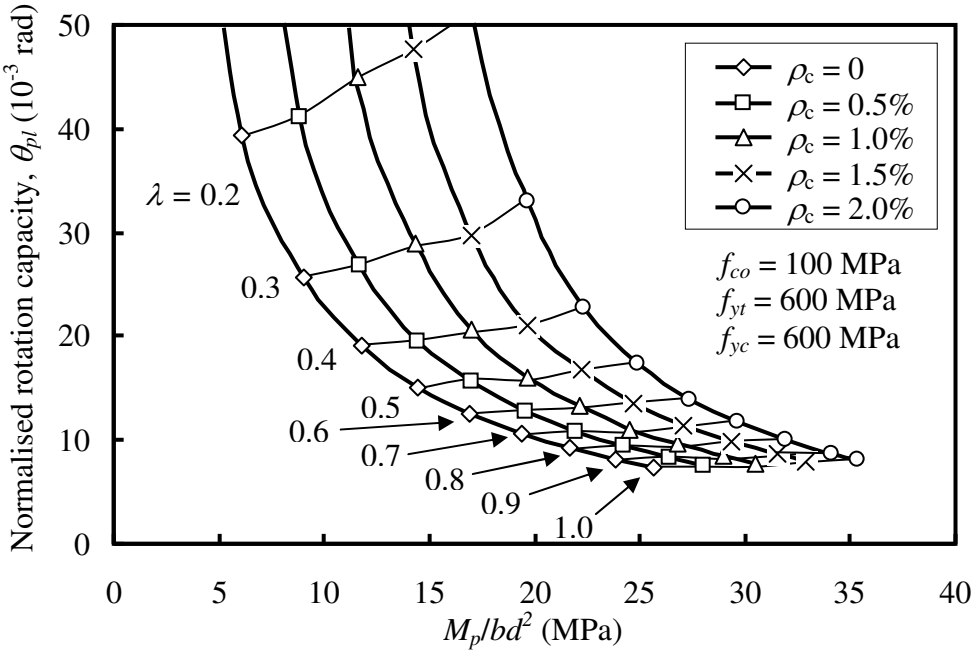

(d) f_{co} = 100 MPa, $f_{yt} = f_{yc}$ = 600 MPa

Figure 8 Design charts for beams with different compression steel ratios

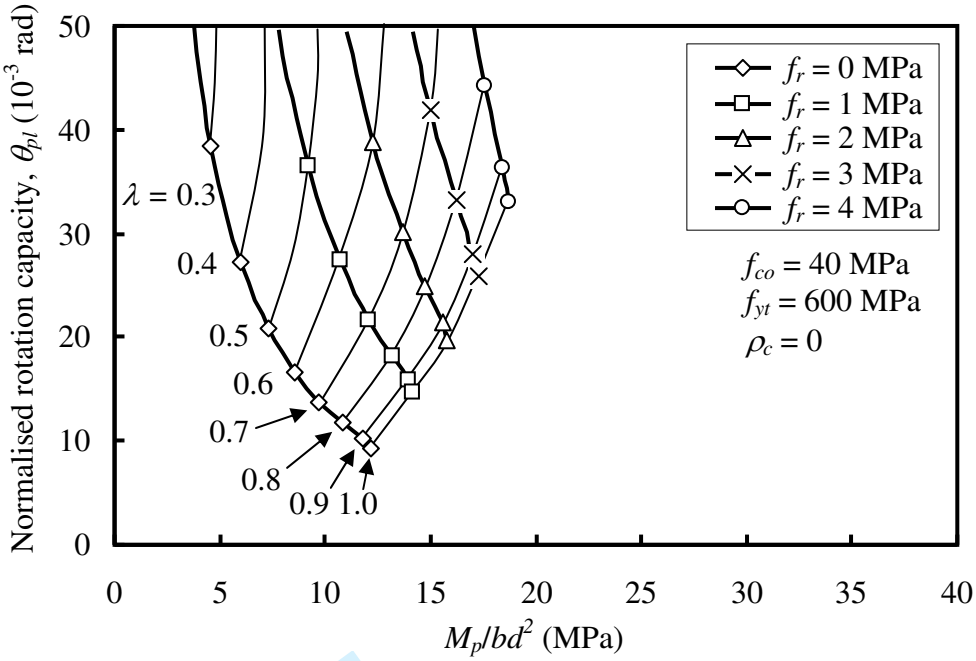

(a) f_{co} = 40 MPa, f_{yt} = 600 MPa

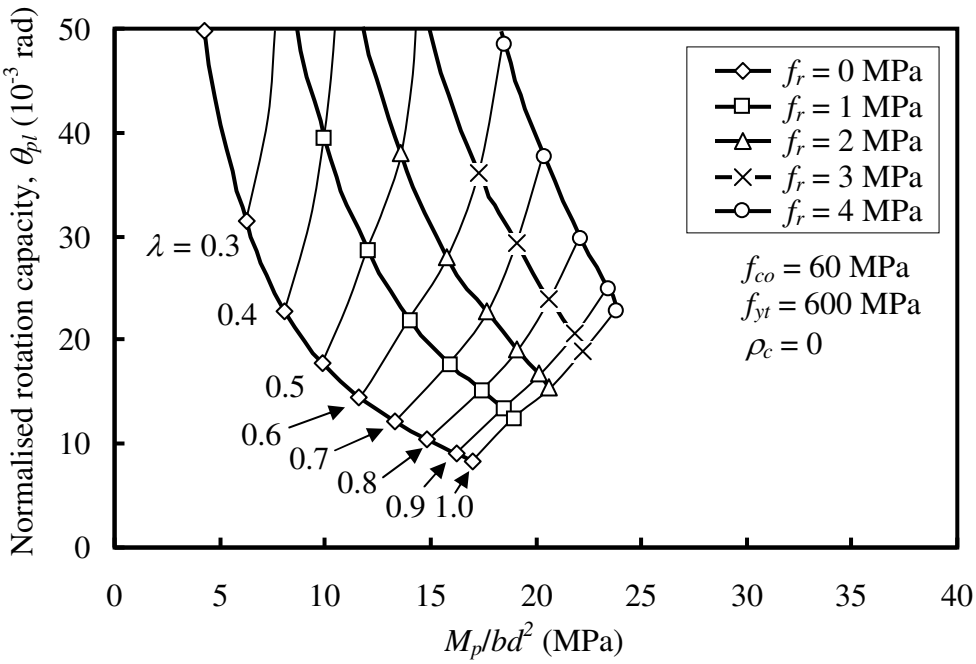

(b) f_{co} = 60 MPa, f_{yt} = 600 MPa

Figure 9 Design charts for beams with different confining pressure

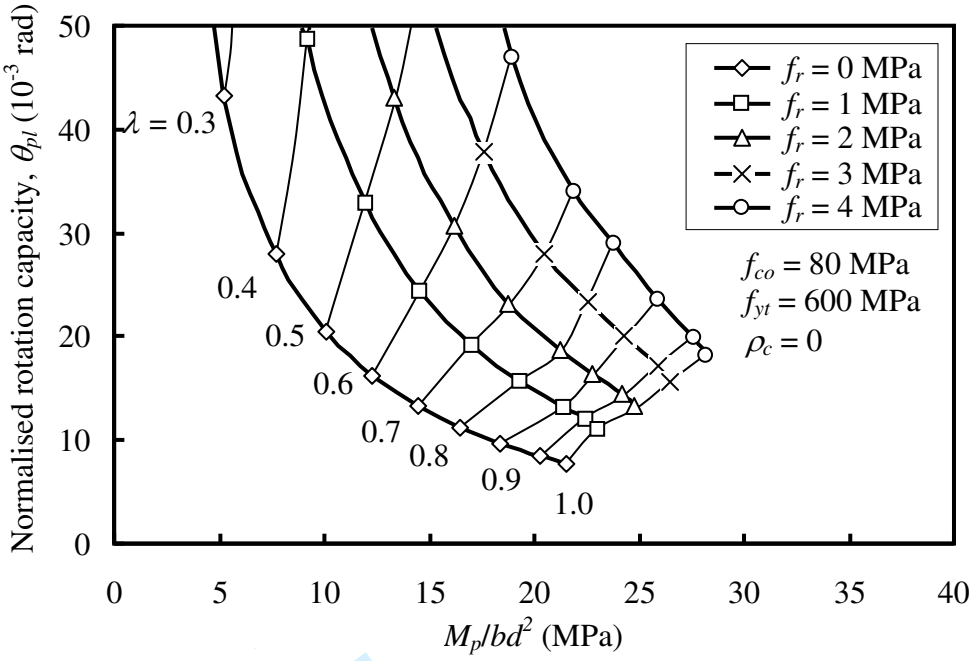

(c) f_{co} = 80 MPa, f_{yt} = 600 MPa

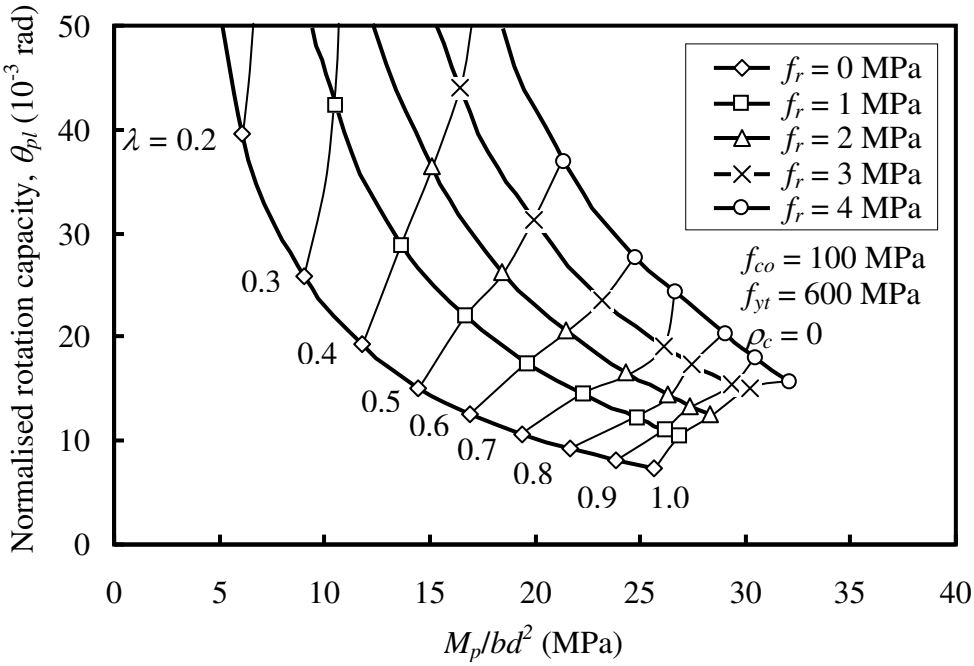

(d) f_{co} = 100 MPa, f_{yt} = 600 MPa

Figure 9 Design charts for beams with different confining pressure